Frontiers of Physics
https://doi.org/10.1007/s11467-020-1010-4
Front. Phys.
15(6), 61501 (2020)

RESEARCH ARTICLE

# On-chip multiphoton Greenberger–Horne–Zeilinger state based on integrated frequency combs

**Pingyu Zhu[1], Qilin Zheng[1], Shichuan Xue[1], Chao Wu[1], Xinyao Yu[1], Yang Wang[1], Yingwen Liu[1], Xiaogang Qiang[2,1], Junjie Wu[1], Ping Xu[1,3,†]**

[1] *Institute for Quantum Information and State Key Laboratory of High Performance Computing, College of Computer, National University of Defense Technology, Changsha 410073, China*
[2] *National Innovation Institute of Defense Technology, AMS, Beijing 100071, China*
[3] *National Laboratory of Solid State Microstructures and School of Physics, Nanjing University, Nanjing 210093, China*
*Corresponding author. E-mail: [†]pingxu520@nju.edu.cn*
*Received September 3, 2020; accepted September 21, 2020*

One of the most important multipartite entangled states, Greenberger–Horne–Zeilinger state (GHZ), serves as a fundamental resource for quantum foundation test, quantum communication and quantum computation. To increase the number of entangled particles, significant experimental efforts should been invested due to the complexity of optical setup and the difficulty in maintaining the coherence condition for high-fidelity GHZ state. Here, we propose an ultra-integrated scalable on-chip GHZ state generation scheme based on frequency combs. By designing several microrings pumped by different lasers, multiple partially overlapped quantum frequency combs are generated to supply as the basis for on-chip polarization-encoded GHZ state with each qubit occupying a certain spectral mode. Both even and odd numbers of GHZ states can be engineered with constant small number of integrated components and easily scaled up on the same chip by only adjusting one of the pump wavelengths. In addition, we give the on-chip design of projection measurement for characterizing GHZ states and show the reconfigurability of the state. Our proposal is rather simple and feasible within the existing fabrication technologies and we believe it will boost the development of multiphoton technologies.

**Keywords** quantum information, Greenberger–Horne–Zeilinger state, frequency comb

## 1 Introduction

Quantum entanglement [1] is a unique property of quantum system and plays as a central role in quantum technologies. The Greenberger–Horne–Zeilinger (GHZ) state, is an entangled quantum state having extremely nonclassical properties [2], with applications including but not limited to the test of local realism [3], quantum error correction [4, 5], authentication [6] and quantum teleportation [7, 8]. With the significantly improved ability of controlling interference and generating multiparticle entanglement [9], experiments in bulk optics successively broke the record for the number of entangled paricles [10, 11] and the experiment up to twelve photons have been demonstrated [12]. Moreover, hyper-entangled states whose qubits are formed in multiple degrees of freedom (DOFs) has been exploited [13] and the GHZ state with more than two levels has been experimental implemented [14] in bulk optics. Quantum photonic chip [15, 16], as an emerging technology, which integrates massive miniature components [17, 18] within several square centimeters, leads to a significant development of optical systems with spatial scalability and phase stability beyond bulk optics [19]. Recently, on-chip schemes for spatially separated multiphoton states including GHZ states were proposed [20–22].

In previous bulk optics and on-chip strategies, each qubit in GHZ state locates in different spatial modes, usually $O(n)$ spontaneous parametric down conversion (SPDC) crystals [10–12] or spontaneous four-wave mixing (SFWM) sources [20–22] are required for an n-qubit GHZ state generation. More nonlinear sources and linear optical components are required as well as incremental length conditions of paths need to be satisfied for ensuring the coherence for high-fidelity GHZ state with more photons, thus the optical system for large photon number GHZ state is complex and not easily engineered. In this work, we make use of spectral modes instead of the spatial modes to simplify the design of GHZ state. Frequency comb which supply the correlations between a large number of frequency bins can be easily achieved by non-degenerate SFWM process in on-chip micro-ring [23, 24]. It has been

*Selected for a View & Perspective. This article can also be found at http://journal.hep.com.cn/fop/EN/10.1007/s11467-020-1010-4.

© Higher Education Press 2020

already used for the construction of complex continuous-variable entanglement between spectral modes [25, 26].

Here we propose an ultra-integrated scalable on-chip GHZ state generation scheme based on frequency combs which not only significantly lower down the spatial complexity for GHZ state but also support long-distance transmission of such state with nowadays dense wavelength division multiplexing (DWDM) technologies. By designing several microrings pumped by different lasers, multiple partially overlapped quantum frequency combs are generated to supply as the basis for on-chip polarization encoded GHZ state with each qubit lying in a specific spectral mode. Both even and odd numbers of GHZ states can be engineered with constant small number of integrated components and easily scaled up on the same chip by only adjusting one of the pump wavelengths. In addition, we give the on-chip design of projection measurement for characterizing GHZ states and show the reconfigurability of the state. Our proposal is rather simple and feasible within the existing fabrication technologies, supplying a new method for multiphoton entangled states which will boost the development of multiphoton technologies.

## 2 Scheme

For constructing GHZ states, it is necessary to introduce a recent striking theory that quantum experiments for the multiphoton entanglement can be related to the perfect matching problem in graph theory [27]. In this theory, optical setups are explained by the undirected graph that down-conversion photon pairs are regarded as edges and output paths are vertices. Then the perfect matchings correspond to the multiphoton terms after the post-selection detection that every output path has one and only one photon [28]. Such theory gives an interesting way to guide the design of quantum experiments and a series of schemes for multiphoton entangled states were proposed [29, 30]. All the experimentally realized GHZ states can be explained by such theory. For example, as shown in

**Table 1** The analogies between graph theory and our spectral-separated experiments for GHZ states.

| Graph theory | Spectral-separated experiments for GHZ states |
|---|---|
| Undirected Graph | Optical chip with micro-ring resonators |
| Vertex | Spectral mode |
| Edges | Frequency-bin pairs in the frenquency comb from micro-ring resonator |
| Colors of the edge (blue, red, black) | Encode numbers ($\|0\rangle$, $\|1\rangle$, $\|2\rangle$) |
| Perfect matching | $n$-fold coincidence of specific spectral modes |
| #(perfect matching) | #(terms of GHZ state) |

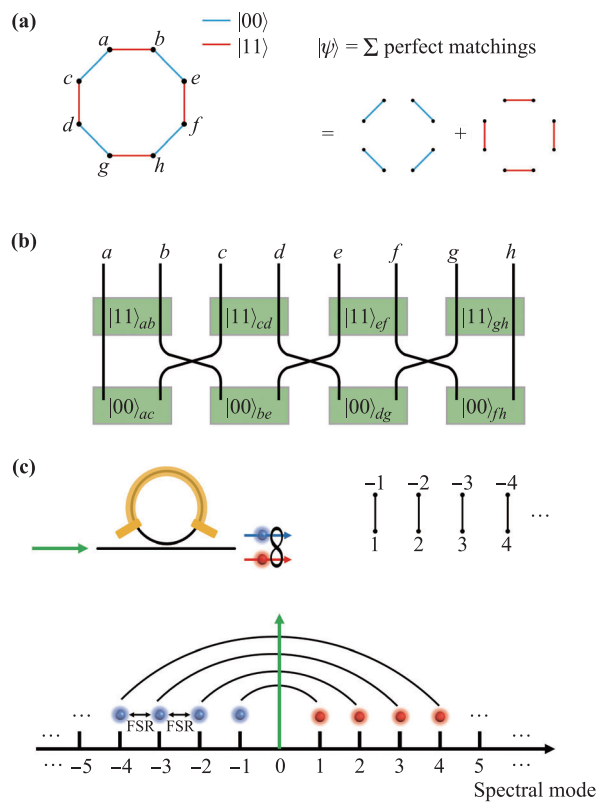



**Fig. 1** **(a)** The graph and **(b)** the corresponding bulk-optical experiment with eight nonlinear crystals for the 2-dimensional 8-photon GHZ state [30]. **(c)** Photon pairs are produced by the SFWM process in an on-chip micro-ring, and they can be used as edges for constructing graphs.

Figs. 1(a) and (b), the graphs for the eight-photon GHZ state is a cycle graph with eight edges that every vertex is connected by two edges encoded in $|0\rangle$ and $|1\rangle$, respectively [30]. In the corresponding quantum experiment of this graph, eight nonlinear crystals are pumped coherently and the pump laser is set at a reasonable power. In the post-selection condition that each output has one and only one photon, the final eight photon GHZ state is obtained. For constructing the graph of an n-qubit GHZ state, $O(n)$ nonlinear two-photon sources are required and $O(n)$ length conditions between optical paths should be satisfied [10–12, 20–22].

Our strategy is to construct the graph for GHZ state by frequency combs in which the paired frequency bins serve as the edges and the spectral modes stand for the graph's vertices. The frequency DOF is naturally high-dimensional and multiple edges can be obtained from a single nonlinear two-photon source, thus it is easy to scale up the graph without increasing the spatial complexity of the optical design. It is worth noting here the frequency DOF is not used for qubit encoding and it is an auxiliary DOF. Our target GHZ state is encoded in polarization. Table 1 lists the correspondence between the graph theoretical concepts and the experimental concepts.

The main element in our proposal is the micro-ring resonator, providing the required frequency comb. The rings on $\chi^{(3)}$ silicon-on-insulator (SOI) with a same radius are considered to be the workhorse. They have a same free spectral range (FSR), i.e., the frequency difference between the resonances. As shown in Fig. 1(b), during the process of non-degenerate SFWM, two pump photons at spectral mode $w_0$ are converted into a signal photon at one of modes $w_1, w_2, w_3, \ldots$ and an idler photon at corresponding spectral mode $w_{-1}, w_{-2}, w_{-3}, \ldots$ by obeying the conservation of energy. These frequency pairs form a quantum frequency comb centered on the spectral mode of pump laser can be used to construct the multiphoton graph. The productivity and quality of the converted photons from rings can be optimized by adding interferometers [31–34]. For simplicity, we just choose the basic micro-ring structure in this paper.

The main structure of our design contain three rings $R_1$, $R_2$, and $R_3$, and the phase shifters on these rings are used to shift their transmission peaks. We install ring $R_1$ to be coupled to the upper waveguide and two rings $R_2$ and $R_3$ in series to be coupled to the lower waveguide as shown in Fig. 2(a). Three coherent pulse pumps A, B and C in a common clock cycle with different frequencies $w_a$, $w_b$ and $w_c$ are required. Pump A and Pump B are directly injected into the upper and the lower waveguide and then each of them leads to a SFWM process in ring $R_1$ and $R_2$, respectively. Next, the Pump B should be filtered out, and simultaneously, the Pump C should be redirected to the lower waveguide. An add-drop filter ring F is a good choice for such purpose whose FSR is twice than the working rings'. Then the Pump C injects into ring $R_3$ for another SFWM process.

Our design guarantees that three rings can be pumped independently by different pump lasers but also coherently that converted photons from different rings are temporal indistinguishable. Each pump laser leads to a quantum frequency comb containing multiple paired frequency bins. The frequency comb from $R_1$ serves as the $|00\rangle$ edges and the frequency comb from $R_2$ together with one frequency pair from $R_3$ shape the graph's $|11\rangle$ edges. The frequency combs are designed in such rule that each spectral mode

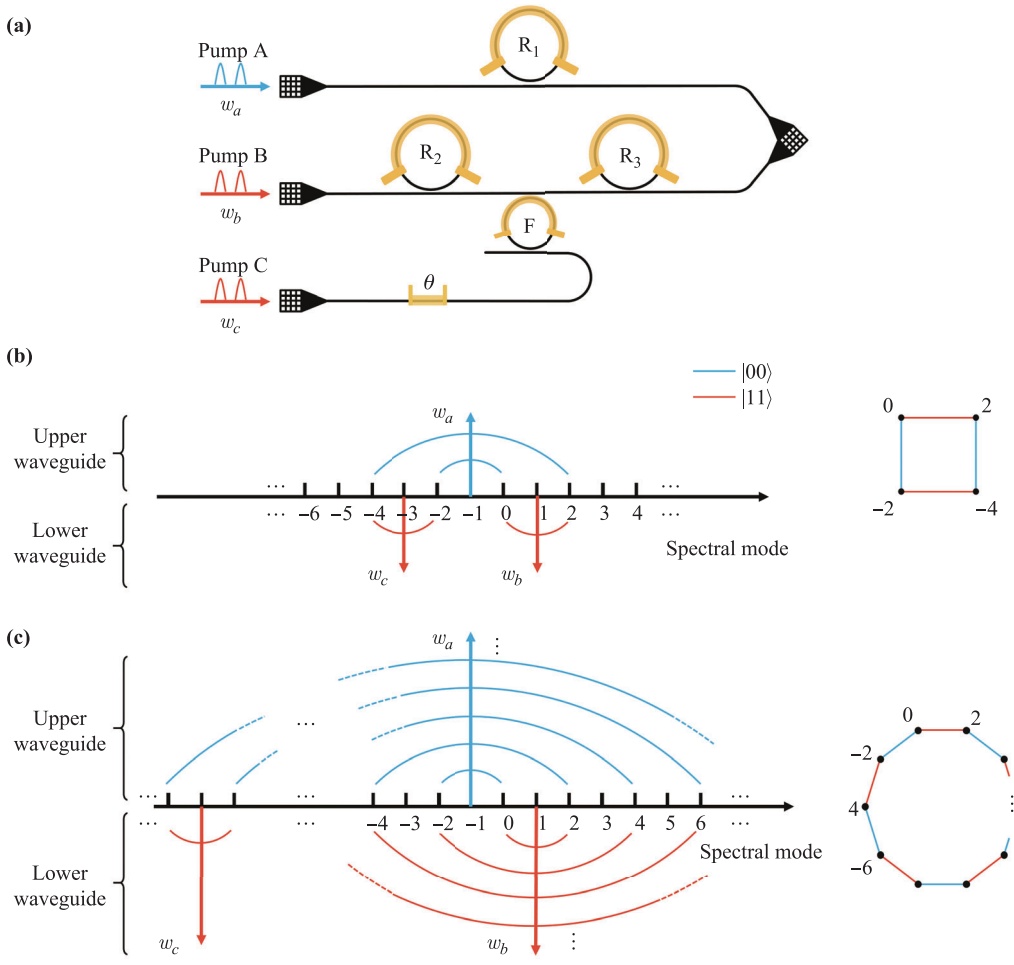



**Fig. 2** **(a)** Scheme of an on-chip structure to generate spectral separated GHZ states with even photons. The spectral settings of pumps and general graphs for producing 2-dimensional **(b)** 4- and **(c)** $n$-particle GHZ states ($n$ is even).

is both generated from upper ring $R_1$ and from lower ring $R_2$ or $R_3$. Thus each qubit occupies only one spetral mode and the encoded $|0\rangle$ or $|1\rangle$ is discriminated by upper (u) or lower (l) waveguide and finally by the horizontal (H) or vertical (V) polarization after the cascaded path-to-polarization converter as shown in Fig. 2(a). The target GHZ state is obtained based on the post-selection detection at specified spectral modes. We take the setting of pumps for four-photon GHZ state in Fig. 2(b) for the example, the superposition state of two-photon terms (photon pairs) after three SFWM processes can be expressed by

$$|\psi\rangle = g\left(|uu\rangle_{-2,0} + |uu\rangle_{-4,2} + \mathrm{e}^{2\mathrm{i}\theta}|ll\rangle_{-4,-2} + |ll\rangle_{0,2}\right), \quad (1)$$

that a photon in upper (lower) waveguide is expressed as $|u\rangle$ ($|l\rangle$). The subscripts represent the spectral mode where the photons locate at. As an example, $|ll\rangle_{-2,0}$ means that the two photons exist in the upper waveguide at spectral modes $w_{-2}$ and $w_0$ respectively. And $g$ stands for the two-photon state's amplitude which absorbs all the constants relating the pump power, nonlinear coefficients and the ring's parameters. In the next stage, a two-dimensional (2D) grating coupler [35, 36] is set as a path-to-polarization conversion interface. Photons from two waveguide are combined into one spatial mode out of the chip via the 2D grating coupler. Photons from upper waveguide are vertically polarized and others from lower waveguide are horizontally polarized when shoot out of the chip to the free space or fiber (i.e., $|u\rangle \to |H\rangle$ and $|l\rangle \to |V\rangle$). So far, the final polarization-encoded four-photon GHZ state is prepared in the single spatial mode when every specified spectral mode ($w_{-4}$, $w_{-2}$, $w_0$, $w_2$ for this exemplified setting) has one and only one photon:

$$\begin{aligned}|\psi\rangle &= g^2\left(|HH\rangle_{-2,0} + |HH\rangle_{-4,2} + \mathrm{e}^{2\mathrm{i}\theta}|VV\rangle_{-4,-2} \right.\\ &\quad \left. + |VV\rangle_{0,2}\right)^2\\ &= g^2\left(|HHHH\rangle_{-4,-2,0,2} + \mathrm{e}^{2\mathrm{i}\theta}|VVVV\rangle_{-4,-2,0,2}\right)\\ &\quad + |\psi_{\mathrm{discard}}\rangle\,. \end{aligned} \quad (2)$$

The state $|\psi_{discard}\rangle$ contains the four-photon states which will be discarded by the post-selection detection. The relative phase between the final two target terms depends on the ring positions and the phase difference between three pumps [37]. A phase shifter on the additional waveguide in the configuration of Fig. 2(b) allows one to give a turnable phase $\theta$ to Pump C. It should be noted that SFWM is quadratic in the pump field, thus the phase of the two-photon states depends on twice the phase of the phase shifter. As an example, we plot the density matrices for $\theta = 0$ and $\theta = \pi/2$ in Figs. 3(a) and (b). However, the phase shifter can also be arranged in the upper or lower waveguide and it will lead to a larger effect on the relative phase. Actually, two-photon states do not have a constant amplitude, even though they from a same comb. But they will combine into two final terms in GHZ state and the relative amplitude between two terms can be adjusted easily by changing the power of any one of the pumps.

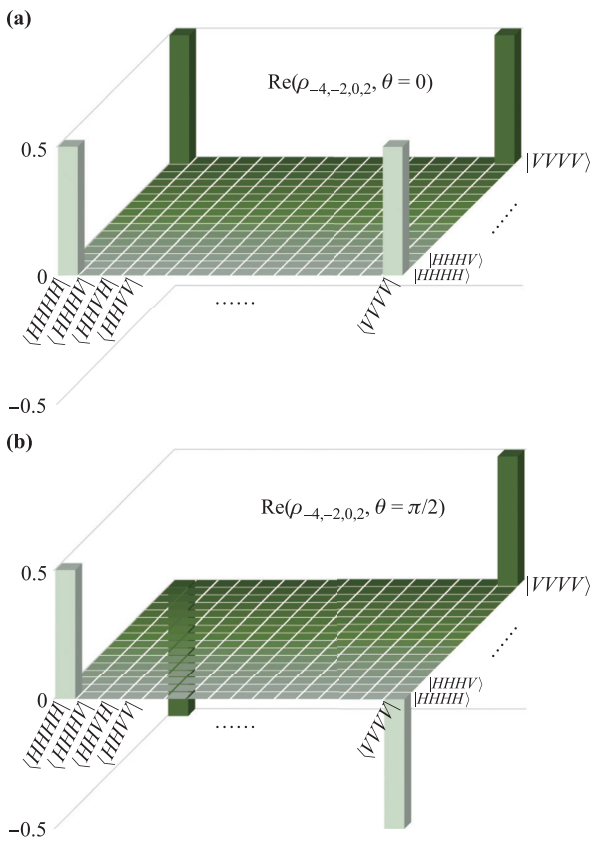



**Fig. 3** Real part of the density matrix of the state generated in the case of **(a)** $\theta = 0$ and **(b)** $\theta = \pi/2$. The imaginary part of density matrix is zero in both examples.

We unfold the graphs to a general form shown in the right of Fig. 2(b) for intuitive understanding. A four-fold coincidence at the four modes $w_{-4}$, $w_{-2}$, $w_0$, $w_2$ can be seen as a subset of edges that contains every vertex only once, which is a perfect matching in the graph. Thus, the coherent superposition of two perfect matchings forms the final GHZ state. This scheme is scalable in terms of the number of qubits. As shown in Fig. 2(c), for adjusting the scale of the state, one just need to change the frequency of Pump C ($w_c$) and add specific new spectral modes in the post-selection detection, without any modifications in the structure of chip. The maximal scale of the state is determined by the number of usable spectral modes in practical experiment. And as we can see, for the large-scale GHZ states, the frequency combs produced by Pump A and Pump B contributes almost all of the edges and the comb from Pump C is responsible for closing the loop in the graph by adding the last missing edge.

Only GHZ states with an even number of photons are attainable by the scheme in Fig. 2. Further inspired by the theory [38] which connects quantum experiments to the perfect matching of hypergraphs (the special graphs

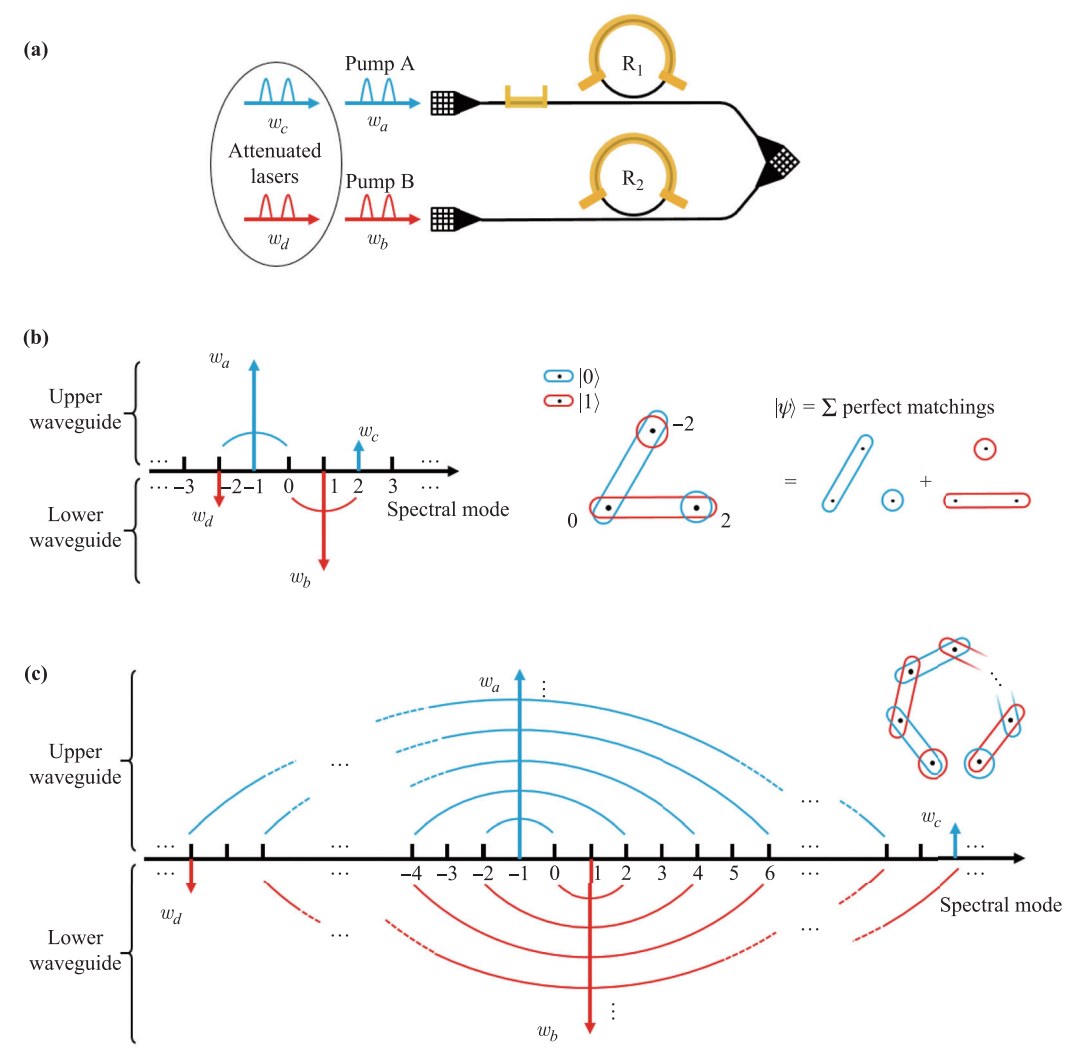



**Fig. 4** **(a)** Scheme of the on-chip structure to generate spectral separated GHZ states with odd photons. The general hypergraphs and the spectral settings of pumps and attenuated lasers for producing 2-dimensional **(b)** 3- and **(c)** $m$-particle GHZ states ($m$ is odd).

with hyperedges connecting an arbitrary number of vertices instead of only two), we further propose a similar on-chip scheme for the GHZ states with an odd number of photons. Pump A at $w_a$ mode and an attenuated laser at modes $w_c$ are directly injected into the upper waveguide, simultaneously Pump B at $w_b$ mode and an attenuated laser at mode $w_d$ are injected into the lower waveguide [Fig. 4(a)]. The attenuated laser beam with low power is approximate to the single photon whose probability is controlled by an attenuator. After SFWM processes, two waveguides are combined by a 2D grating coupler. The spectral modes where the pumps, attenuated lasers and photon pairs at for three-photon GHZ state are shown in Fig. 4(b). The state is obtained when every specified mode (modes $w_{-2}$, $w_0$, $w_2$) have one and only one photon. The photon pairs from two frequency combs produced in ring $R_1$, $R_2$ are represent by the hyperedges connecting two spectral modes and the single photon from attenuated laser corresponds to the hyperedges connecting only one vertex. Only the two perfect matchings of the hypergraph may contribute to the final three-fold coincidence after post-selection, and they forms the final state: $|HHH\rangle_{-2,0,2} + |VVV\rangle_{-2,0,2}$. Similar to the first scheme, the GHZ state with odd photons can also be extended to more photons by moving the frequency of two attenuated lasers as shown in Fig. 4(c).

These states can be verified by quantum state tomography [39], witness operator [40] or other methods [41] via projection measurement. Before the projection for every qubit, a wavelength division multiplexer(WDM) should be arranged to separate the polarization-encoded qubits at different spectral modes into specific paths respectively [see Fig. 5(a)]. And then each qubit of the state can be projected on an arbitrary polarization basis by adjusting

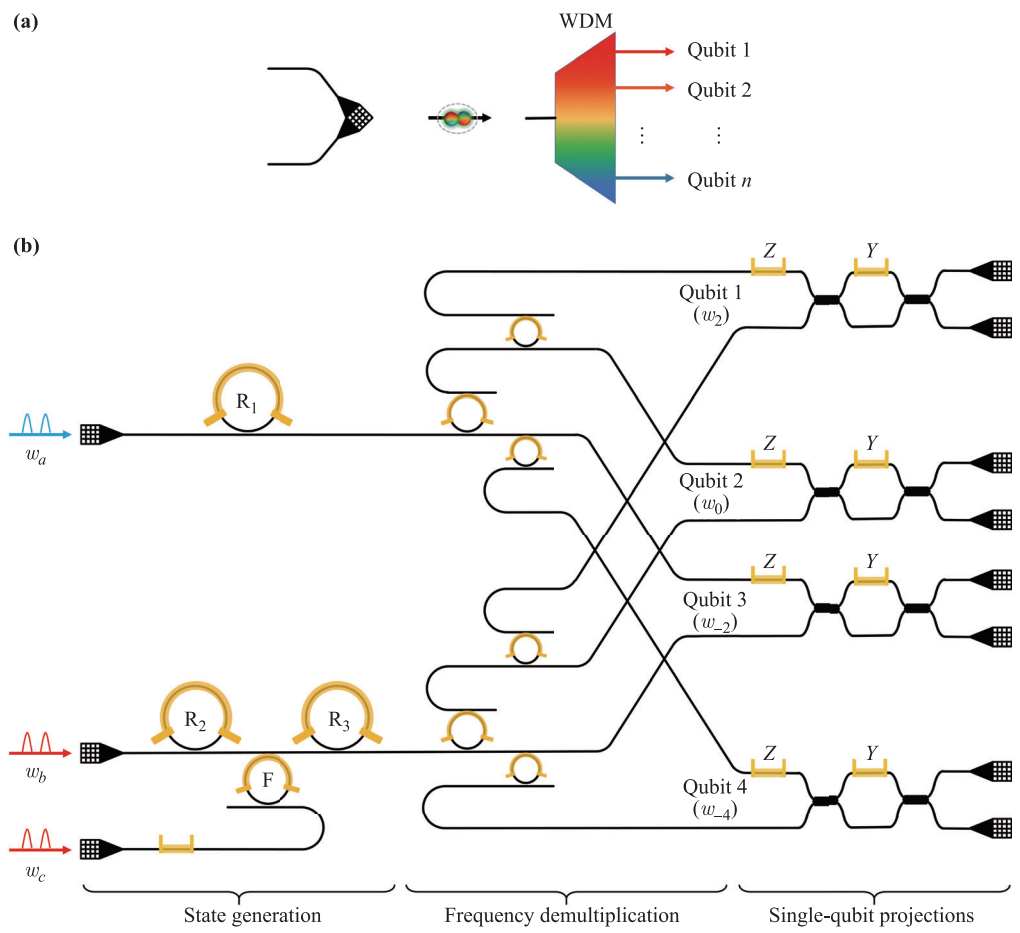



**Fig. 5** The off-chip device **(a)** and on-chip structure **(b)** for verification and computation of the 2-dimensional spectral separated GHZ state.

the common elements including a quarter-wave plate, a half wave plate and a polarization beam splitter before the detector. We also give an alternative approach to measure these states on chip with higher integration and better stability. As shown in Fig. 5(b), in our scheme, the photons with distinct frequency from upper or lower waveguides are separated into specific paths by multi-layer rings, that the FSR of first layer rings is four times as long as the core rings and then the FRS of each ring layer is doubled in succession. It is not the only choice of on-chip WDM and the asymmetric Mach–Zenhder interferometer network can also be used for such frequency demultiplexing task. After frequency demultiplexing, path-encoded GHZ state is formed by the superposition of states that every qubit has one and only one photon. Then, the path-encoded single-qubit projections are set with a phase shifter controlling the rotation angle of $Z$ direction and a Mach–Zehnder interferometer (MZI) implementing the $Y$ rotation respectively.

In addition, we find our method can also generate the 3-dimensional four-photon GHZ state. Compared to the previous structure in Fig. 2(a), the scheme for the 3-dimensional four-photon GHZ state has one more waveguide which coupled two new rings $R_4$ and $R_5$, as shown in Fig. 6. Five pumps at spectral modes $w_a$, $w_b$, $w_c$, $w_d$, $w_e$ respectively pumped in Ring $R_1$, $R_2$, $R_3$, $R_4$, $R_5$ independently and coherently. The frequency setting of pumps is shown in Fig. 6(b). We only consider the converted photon pairs at specified spectral modes $w_{-4}$, $w_{-2}$, $w_2$, $w_4$ which construct a graph with six edges. Two-photon states produced in the first, the second and the third waveguides denote as $|00\rangle$, $|11\rangle$, $|22\rangle$, respectively. However, in order to combine the photons from these three paths, we should find a new interface between spatial DOF and another high-dimensional DOF (such as time [42] and orbital angular momentum) rather than 2D grating. After the transformation from path to the high-dimensional DOF, the coherent superposition of the states that every specified mode ($w_{-4}$, $w_{-2}$, $w_2$, $w_4$) has one and only one photon construct the 3-dimensional four-photon state. This state can also be verified or be used for computation by on-chip spatial projection. Similar with the aforementioned on-chip projection measurement, multi-layer rings are arranged for frequency demultiplexing at first and then the

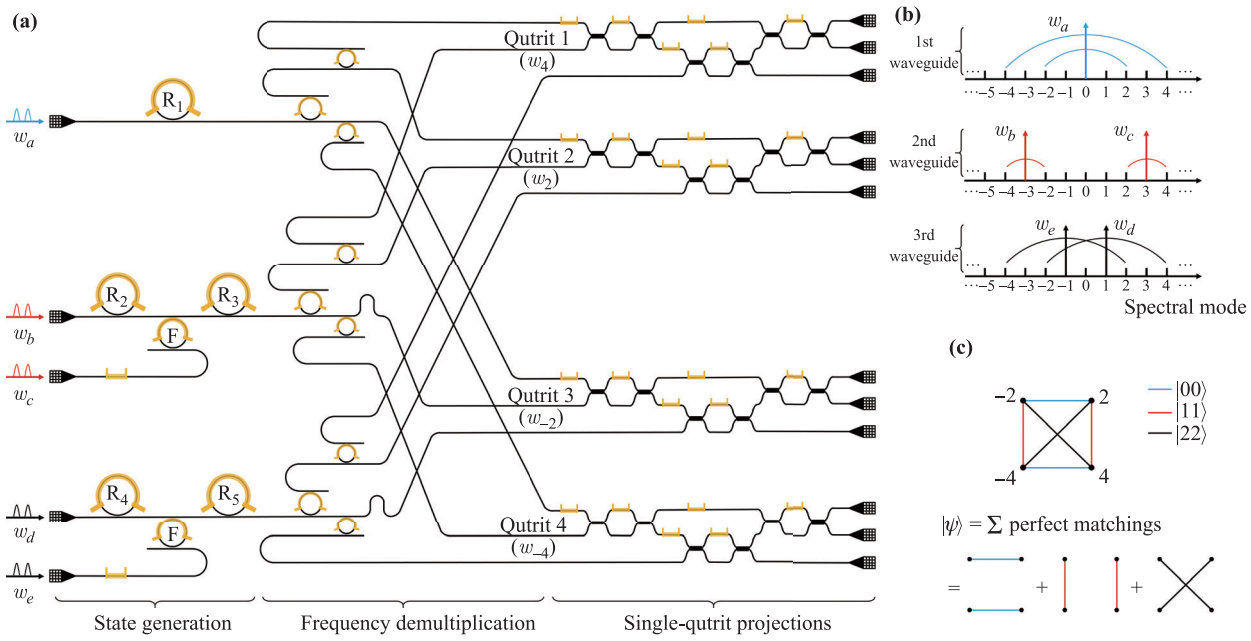



**Fig. 6** **(a)** The scheme, **(b)** the spectral settings of pumps and **(c)** corresponding graph for the generation and verification of 3-dimensional 4-photon spectral separated GHZ state.

state become path-encoded whose qutrits can be projected arbitrarily by the three-dimensional multiport made up by three MZIs and three phase shifters [43, 44].

## 3 Conclusion

In this paper, we propose a systematic solution for ultra-integrated and scalable generation of GHZ states including the even and odd number and the three-dimensional 4-photon GHZ state, taking advantages of frequency combs. The main advantages of our strategy include: i) simplicity and scalability. Several sets of quantum frequency comb from micro-rings serves as the key resources and one can scale up the state to more photons on the same chip. ii) Phase stability and reconfigurability which are the natural advantages of quantum photonic chips. iii) Low spatial cost of transmission. In above schemes, two parts i.e., GHZ state generation and state characterization can both be integrated in a single chip for local realism test or computation, or can be split into two far-separated chips linking only by a single-mode fibre or free space to support long-distance quantum tasks such as the point-to-multipoint quantum secret sharing [45], quantum secure direct communication [46], the entanglement-based wavelength multiplexed quantum communication network [47] and the blind quantum computation [48, 49]. We believe that our idea, which distinguish the photon's labels in frequency domain, have potentials for generating more complex states. The technology of the operations between spectral modes [50–52] and a weight optimization algorithm for the generalized graphs [53] may be helpful for further designs.

**Acknowledgements** This work was supported by the National Basic Research Program of China (973 Program) (Grand Nos. 2017YFA0303700 and 2019YFA0308700), the National Natural Science Foundation of China (Grant Nos. 61632021, and 11690031), and Open Funds from the State Key Laboratory of High Performance Computing of China (HPCL, National University of Defense Technology).

## References

1. A. Einstein, B. Podolsky, and N. Rosen, Can quantum-mechanical description of physical reality be considered complete? *Phys. Rev.* 47(10), 777 (1935)
2. D. M. Greenberger, M. A. Horne, A. Shimony, and A. Zeilinger, Bell's theorem without inequalities, *Am. J. Phys.* 58(12), 1131 (1990)
3. J. Pan, D. Bouwmeester, M. Daniell, H. Weinfurter, and A. Zeilinger, Experimental test of quantum nonlocality in three-photon Greenberger–Horne–Zeilinger entanglement, *Nature* 403(6769), 515 (2000)
4. A. R. Calderbank and P. W. Shor, Good quantum error correcting codes exist, *Phys. Rev. A* 54(2), 1098 (1996)
5. R. Raussendorf, J. Harrington, and K. Goyal, Topological fault-tolerance in cluster state quantum computation, *New J. Phys.* 9(6), 199 (2007)
6. A. Farouk, J. Batle, M. Elhoseny, M. Naseri, M. Lone, A. Fedorov, M. Alkhambashi, S. H. Ahmed, and M. Abdel-

Aty, Robust general $n$ user authentication scheme in a centralized quantum communication network via generalized GHZ states, *Front. Phys.* 13(2), 130306 (2018)

7. K. Wang, X. T. Yu, and Z. C. Zhang, Two-qubit entangled state teleportation via optimal POVM and partially entangled GHZ state, *Front. Phys.* 13(5), 130320 (2018)
8. X. Hu, C. Zhang, C. Zhang, B. Liu, Y. Huang, Y. Han, C. Li, and G. Guo, Experimental certification for nonclassical teleportation, *Quantum Eng.* 1(2), e13 (2019)
9. J. Pan, Z. Chen, C. Lu, H. Weinfurter, A. Zeilinger, and M. Zukowski, Multi-photon entanglement and interferometry, *Rev. Mod. Phys.* 84(2), 777 (2012)
10. Y. Huang, B. Liu, L. Peng, Y. Li, L. Li, C. Li, and G. Guo, Experimental generation of an eight-photon Greenberger–Horne–Zeilinger state, *Nat. Commun.* 2(1), 546 (2011)
11. X. L. Wang, L. K. Chen, W. Li, H. L. Huang, C. Liu, C. Chen, Y. H. Luo, Z. E. Su, D. Wu, Z. D. Li, H. Lu, Y. Hu, X. Jiang, C. Z. Peng, L. Li, N. L. Liu, Y. A. Chen, C. Y. Lu, and J. W. Pan, Experimental ten-photon entanglement, *Phys. Rev. Lett.* 117(21), 210502 (2016)
12. H. S. Zhong, Y. Li, W. Li, L. C. Peng, Z. E. Su, Y. Hu, Y. M. He, X. Ding, W. Zhang, H. Li, L. Zhang, Z. Wang, L. You, X. L. Wang, X. Jiang, L. Li, Y. A. Chen, N. L. Liu, C. Y. Lu, and J. W. Pan, 12-photon entanglement and scalable scattershot boson sampling with optimal entangled-photon pairs from parametric down-conversion, *Phys. Rev. Lett.* 121(25), 250505 (2018)
13. X. L. Wang, Y. H. Luo, H. L. Huang, M. C. Chen, Z. E. Su, C. Liu, C. Chen, W. Li, Y. Q. Fang, X. Jiang, J. Zhang, L. Li, N. L. Liu, C. Y. Lu, and J. W. Pan, 18-qubit entanglement with six photons' three degrees of freedom, *Phys. Rev. Lett.* 120(26), 260502 (2018)
14. M. Erhard, M. Malik, M. Krenn, and A. Zeilinger, Experimental Greenberger–Horne–Zeilinger entanglement beyond qubits, *Nat. Photonics* 12(12), 759 (2018)
15. Q. Zhang, P. Xu, and S. Zhu, Quantum photonic network on chip, *Chin. Phys. B* 27(5), 054207 (2018)
16. J. Wang, F. Sciarrino, A. Laing, and M. G. Thompson, Integrated photonic quantum technologies, *Nat. Photonics* 14(5), 273 (2020)
17. X. Qiang, X. Zhou, J. Wang, C. M. Wilkes, L. Thomas, O. Sean, K. Laurent, G. D. Marshall, S. Raffaele, and T. C. Ralph, Large-scale silicon quantum photonics implementing arbitrary two-qubit processing, *Nat. Photonics* 12(9), 534 (2018)
18. J. Wang, S. Paesani, Y. Ding, R. Santagati, P. Skrzypczyk, A. Salavrakos, J. Tura, R. Augusiak, L. Mančinska, D. Bacco, D. Bonneau, J. W. Silverstone, Q. Gong, A. Acín, K. Rottwitt, L. K. Oxenløwe, J. L. O'Brien, A. Laing, and M. G. Thompson, Multidimensional quantum entanglement with large-scale integrated optics, *Science* 360(6386), 285 (2018)
19. R. Terry, Why I am optimistic about the silicon-photonic route to quantum computing, *APL Photonics* 2, 030901 (2016)
20. T. Feng, X. Zhang, Y. Tian, and Q. Feng, On-chip multi-photon entangled states by path identity, *Int. J. Theor. Phys.* 58(11), 3726 (2019)
21. J. C. Adcock, C. Vigliar, R. Santagati, J. W. Silverstone, and M. G. Thompson, Programmable four-photon graph states on a silicon chip, *Nat. Commun.* 10(1), 3528 (2019)
22. P. Zhu, S. Xue, Q. Zheng, C. Wu, X. Yu, Y. Wang, Y. Liu, X. Qiang, M. Deng, J. Wu, and P. Xu, Reconfigurable multiphoton entangled states based on quantum photonic chips, *Opt. Express* 28(18), 26792 (2020)
23. M. Kues, C. Reimer, P. Roztocki, L. R. Cortes, S. Sciara, B. Wetzel, Y. Zhang, A. C. Cino, S. T. Chu, B. E. Little, D. J. Moss, L. Caspani, J. Azaña, and R. Morandotti, On-chip generation of high-dimensional entangled quantum states and their coherent control, *Nature* 546(7660), 622 (2017)
24. C. Reimer, M. Kues, P. Roztocki, B. Wetzel, F. Grazioso, B. E. Little, S. T. Chu, T. W. Johnston, Y. Bromberg, L. Caspani, D. J. Moss, and R. Morandotti, Generation of multi-photon entangled quantum states by means of integrated frequency combs, *Science* 351(6278), 1176 (2016)
25. M. Chen, N. C. Menicucci, and O. Pfister, Experimental realization of multipartite entanglement of 60 modes of a quantum optical frequency comb, *Phys. Rev. Lett.* 112(12), 120505 (2014)
26. B. H. Wu, R. N. Alexander, S. Liu, and Z. Zhang, Quantum computing with multidimensional continuous-variable cluster states in a scalable photonic platform, *Phys. Rev. Research* 2(2), 023138 (2020)
27. M. Krenn, X. Gu, and A. Zeilinger, Quantum experiments and graphs: Multiparty states as coherent super-positions of perfect matchings, *Phys. Rev. Lett.* 119(24), 240403 (2017)
28. E. Knill, R. Laflamme, and G. J. Milburn, A scheme for efficient quantum computation with linear optics, *Nature* 409(6816), 46 (2001)
29. X. Gu, M. Erhard, A. Zeilinger, and M. Krenn, Quantum experiments and graphs (ii): Quantum interference, computation, and state generation, *Proc. Natl. Acad. Sci. USA* 116(10), 4147 (2019)
30. X. Gu, L. Chen, A. Zeilinger, and M. Krenn, Quantum experiments and graphs (iii): High-dimensional and multiparticle entanglement, *Phys. Rev. A* 99(3), 032338 (2019)
31. C. Wu, Y. Liu, X. Gu, S. Xue, X. Yu, Y. Kong, X. Qiang, J. Wu, Z. Zhu, and P. Xu, Characterize and optimize the four-wave mixing in dual-interferometer coupled silicon microrings, *Chin. Phys. B* 28(10), 104211 (2019)
32. C. Wu, Y. Liu, X. Gu, X. Yu, Y. Kong, Y. Wang, X. Qiang, J. Wu, Z. Zhu, X. Yang, and P. Xu, Bright photon-pair source based on a silicon dual-Mach–Zehnder microring, *Sci. China Phys. Mech. Astron.* 63(2), 220362 (2020)
33. Y. Liu, C. Wu, X. Gu, Y. Kong, X. Yu, R. Ge, X. Cai, X. Qiang, J. Wu, X. Yang, and P. Xu, High-spectral-purity photon generation from a dual-interferometer-coupled silicon microring, *Opt. Lett.* 45(1), 73 (2020)
34. P. Zhu, Y. Liu, C. Wu, S. Xue, X. Yu, Q. Zheng, Y. Wang, X. Qiang, J. Wu, and P. Xu, Near 100% spectral-purity photons from reconfigurable micro-rings, *Chin. Phys. B* 29, 114201 (2020)

35. D. Taillaert, P. I. Harold Chong, P. I. Borel, L. H. Frandsen, R. M. De La Rue, and R. Baets, A compact two-dimensional grating coupler used as a polarization splitter, *IEEE Photonics Technol. Lett.* 15(9), 1249 (2003)
36. J. Wang, D. Bonneau, M. Villa, J. W. Silverstone, R. Santagati, S. Miki, T. Yamashita, M. Fujiwara, M. Sasaki, H. Terai, M. G. Tanner, C. M. Natarajan, R. H. Hadfield, J. L. O'Brien, and M. G. Thompson, Chip-to-chip quantum photonic interconnect by path-polarization interconversion, *Optica* 3(4), 407 (2016)
37. M. Liscidini and J. E. Sipe, Scalable and efficient source of entangled frequency bins, *Opt. Lett.* 44(11), 2625 (2019)
38. X. Gu, L. Chen, and M. Krenn, Quantum experiments and hypergraphs: Multiphoton sources for quantum interference, quantum computation, and quantum entanglement, *Phys. Rev. A* 101(3), 033816 (2020)
39. D. F. V. James, P. G. Kwiat, W. J. Munro, and A. G. White, Measurement of qubits, *Phys. Rev. A* 64(5), 052312 (2001)
40. O. Gühne and G. Toth, Entanglement detection, *Phys. Rep.* 474(1–6), 1 (2009)
41. X. Chen, L. Jiang, and Z. Xu, Precise detection of multipartite entanglement in four-qubit Greenberger–Horne–Zeilinger diagonal states, *Front. Phys.* 13(5), 130317 (2018)
42. J. Tang, Z. Hou, Q. Xu, G. Xiang, C. Li, and G. Guo, Polarization-independent coherent spatial-temporal interface with low loss, *Phys. Rev. Appl.* 12(6), 064058 (2019)
43. M. Reck, A. Zeilinger, H. J. Bernstein, and P. Bertani, Experimental realization of any discrete unitary operator, *Phys. Rev. Lett.* 73(1), 58 (1994)
44. L. Lu, L. Xia, Z. Chen, L. Chen, T. Yu, T. Tao, W. Ma, Y. Pan, X. Cai, Y. Lu, S. Zhu, and X. S. Ma, Three-dimensional entanglement on a silicon chip, *NPJ Quantum Inf.* 6(1), 30 (2020)
45. L. Xiao, G. Long, F. Deng, and J. Pan, Efficient multiparty quantum-secret-sharing schemes, *Phys. Rev. A* 69(5), 052307 (2004)
46. Z. Man, Y. Xia, and N. B. An, Quantum secure direct communication by using GHZ states and entanglement swapping, *J. Phys. B* 39(18), 3855 (2006)
47. S. Wengerowsky, S. K. Joshi, F. Steinlechner, H. Hubel, and R. Ursin, An entanglement-based wavelength-multiplexed quantum communication network, *Nature* 564(7735), 225 (2018)
48. P. Arrighi and L. Salvail, Blind quantum computation, *Int. J. Quant. Inf.* 04(05), 883 (2006)
49. S. Barz, E. Kashefi, A. Broadbent, J. F. Fitzsimons, A. Zeilinger, and P. Walther, Demonstration of blind quantum computing, *Science* 335(6066), 303 (2012)
50. J. M. Lukens and P. Lougovski, Frequency-encoded photonic qubits for scalable quantum information processing, *Optica* 4(1), 8 (2017)
51. H. H. Lu, J. M. Lukens, N. A. Peters, B. P. Williams, A. M. Weiner, and P. Lougovski, Quantum interference and correlation control of frequency-bin qubits, *Optica* 5(11), 1455 (2018)
52. S. Ramelow, A. Fedrizzi, A. Poppe, N. K. Langford, and A. Zeilinger, Polarization-entanglement-conserving frequency conversion of photons, *Phys. Rev. A* 85(1), 013845 (2012)
53. M. Krenn, J. Kottmann, N. Tischler, and A. Aspuru-Guzik, Conceptual understanding through efficient inverse-design of quantum optical experiments, arXiv: 2005.06443 [quant-ph] (2020)